35th Annual International Conference of the IEEE EMBS
Osaka, Japan, 3 - 7 July, 2013

Registration of Abdominal Tumor DCE-MRI Data Based on Deconvolution of Joint Statistics

David Pilutti*, Martin Büchert, Stathis Hadjidemetriou
University Medical Center Freiburg, 79106 Freiburg, Germany
david.pilutti@uniklinik-freiburg.de

Abstract— **The analysis of Dynamic Contrast Enhanced Magnetic Resonance Imaging (DCE-MRI) data of body tumors presents several challenges. The accumulation of contrast agent in tissues results in a temporally varying contrast in an image series. At the same time, the body regions are subject to potentially extensive motion mainly due to breathing, heart beat, and peristalsis. This complicates any further automated analysis of a DCE-MRI time series such as for tumor lesion segmentation and volumetry. To address this problem we propose a novel effective non-rigid registration method based on the restoration of the joint statistics of pairs of images in the time series. Every image in the time series is registered to a reference one from the contrast enhanced phase. The pairwise registration is performed with deconvolution of the joint statistics, forcing the results back to the spatial domain and regularizing them with Gaussian spatial smoothing. The registration method has been validated with both a simulated phantom as well as real datasets with improved results for both its accuracy and efficiency.**

I. Introduction

DCE-MRI plays an important role for the identification of vital tumors in the abdominal area. The injection of a contrast agent and its temporal accumulation in tissues can highlight anatomic and pathologic structures aiding a medical doctor in lesion identification. The intensity and contrast in DCE-MRI time series varies significantly along time. These variations hold information regarding the state of the vessel system such as perfusion and permeability. The interpretation of the data with sufficient precision to provide information about disease progression and treatment requires automated analysis. This is however hampered by temporal contrast change and by complex physiological movements that may introduce spatial misregistration along time.

Some of the most commonly used methods for DCE-MRI registration are based on B-splines [1] as well as on the Demons method [2] combined with a distance measure such as the mutual information (MI) [3], [4]. However, the MI being only a scalar quantity under-constrains the registration. That makes MI based methods computationally demanding for volumetric datasets and in practice must be combined with considerable spatial subsampling or multiresolution [1], [3], [4].

We propose a novel systematic non-rigid registration method that is based on the deconvolution of the joint statistics of pairs of images in a time series. The registration operates in full image resolution with very limited time requirements. The spatial misregistration is assumed to cause dispersion on the joint statistics [5]. The problem is approached as a statistical deconvolution one, where the effect of the dispersion is represented as a convolution of the statistics and is restored with Wiener filtering [6]. The deconvolved statistics are indexed and enforced to the registration between the images to obtain an initial spatial transformation. Then, the transformation is regularized for smoothness. The proposed method is iterative and has been validated on a variable contrast extension of the 3D Shepp-Logan simulated phantom [7] and 3D+time real datasets of the human liver, lung, and prostate.

*The first author acknowledges the support of the European Commission through the MIBISOC project (MarieCurie Initial Training Network, FP7 PEOPLE-ITN-2008, GA n. 238819)

II. Method

The method developed takes as reference a frame manually selected from the contrast enhanced phase of DCE-MRI. The method first performs rigid and affine registration steps in cascade and uses the result to initialize the subsequent non-rigid registration step. In this work the dispersion of the distributions of the joint statistics is assumed to result from Gaussian smoothing, which is deconvolved with Wiener filtering. This assumes a smoothness of anatomy in space and a larger size for anatomic structures compared to the extent of the motion. The non-rigid registration deconvolves the joint statistics with a Wiener filter to estimate spatial transformations iteratively, $k = 0, ..., K-1$ for a total of K iterations. It also regularizes the transformations with spatial smoothing.

A. Registration of the DCE-MRI time series

The entire DCE-MRI time series has been registered to a reference image selected from the contrast enhanced phase where the lesion contrast and the overall contrast is higher.

A pairwise registration is between a reference image $I_{ref}(\mathbf{x})$ and a moving image $I_{mov}(\mathbf{x})$ taken from a time series of images I_t with $t = 0, ..., \tau - 1$, where τ is the total number of images in the time series and $\mathbf{x} = (x, y, z)$ are the spatial coordinates. A spatial transformation $\mathbf{T} = (u_x, u_y, u_z)$ from I_{ref} to I_{mov} is estimated to obtain a registered image $I_{reg} = I_{mov}(\mathbf{T}^{-1}(\mathbf{x}))$. The problem of the non-rigid registration of pairs of images in a time series is formulated with two priors. The first results from the deconvolution of the joint intensity statistics with the Wiener

filter. The second results from the spatial regularization of the registration with a Gaussian filter. The registration can accommodate a temporally variable contrast. The method allows the registration over a limited Region Of Interest (ROI) of the image for which the contrast is intended for.

B. Wiener deconvolution of joint intensity statistics

Two images I_{ref} and I_{mov} under assumed perfect alignment give rise to the joint histogram H_{ideal}. The joint statistics H_0 of the misregistered images are considered to result from the convolution of H_{ideal} with a 2D Gaussian filter $G_{i,j}$ to give $H_0 = H_{ideal} * G_{i,j}$, where $*$ is the convolution and i, j signify the dynamic ranges of I_{ref} and I_{mov}, respectively. The statistics H_0 are deconvolved with a 2D Wiener filter $f_{i,j} = \frac{G_{i,j}}{||G_{i,j}||_2^2+\epsilon}$, where ϵ assumes a small value. The filter $f_{i,j}$ is convolved with H_0 to obtain an estimate of the deconvolved statistics as $H_{rest} = H_0 * f_{i,j}$. The images in Fig. 1c and 1d are the joint statistics of images in Fig. 1a and 1b at different iterations before the Wiener deconvolution. The deconvolved statistics are used as a prior that constrains the estimation of the registration.

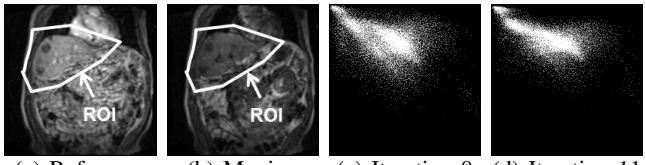

(a) Reference (b) Moving (c) Iteration 0 (d) Iteration 11

Fig. 1: Joint statistics for initial images (a) and (b) before Wiener deconvolution at the initial iteration (c) and after 11 iterations (d). The joint statistics become sharper.

C. Enforcement of priors to the pairwise registration

A graph $R = (V, E)$ is constructed. Each of the vertices in V corresponds to a voxel in the image. The edges in E are connecting each node corresponding to a voxel in I_{ref} to nodes of voxels in spatial neighborhood N in I_{mov}. In I_{mov} we consider the 6-connected neighborhood around every voxel $\mathbf{x}$, $N(\mathbf{x}) = \mathbf{x} + \Delta\mathbf{x}$, where $\Delta\mathbf{x} = (\pm d_x, \pm d_y, \pm d_z)$ and d_x, d_y, d_z are the sizes of a voxel along different axes. The voxel anisotropy is accounted for by using an edge weight $w_d = 1/(d+1)$ for a distance d.

The intensities of the edge between $I_{ref}(\mathbf{x})$ and $I_{mov}(\mathbf{x}+\Delta\mathbf{x})$ form an index for the restored joint histogram to retrieve the second edge weight $w_H = H_{rest}(I_{ref}(\mathbf{x}), I_{mov}(\mathbf{x}+\Delta\mathbf{x}))$. The product $w_{tot}(\mathbf{x}+\Delta\mathbf{x})$, $w_{tot} = w_d \cdot w_H$ gives the total weight of an edge. The linear expectation of the direction of the edges connecting $\mathbf{x}$ over their weights gives an initial displacement $\mathbf{T}''(\mathbf{x})$ for voxel $\mathbf{x}$. At every iteration the displacements over the entire image give an initial transformation

$$\mathbf{T}''_k(\mathbf{x}) = E_{w_{tot}}(\mathbf{x}+\Delta\mathbf{x}) = \frac{\Sigma_N w_{tot}(\mathbf{x}+\Delta\mathbf{x})(\mathbf{x}+\Delta\mathbf{x})}{\Sigma_N w_{tot}(\mathbf{x}+\Delta\mathbf{x})}, \quad (1)$$

that is accumulated to obtain $\mathbf{T}'_k = \mathbf{T}'_{k-1} + \mathbf{T}''_k$. The second prior is the spatial regularization. To regularize the estimation of the transformation $\mathbf{T}'_k$, the gradient magnitude $||\nabla\mathbf{T}'_k||_2$ over the image is penalized, that is equivalent to applying a 3D Gaussian filter $G(\mathbf{x}; \sigma_S)$ to the spatial transformation $\mathbf{T}'_k$ at every iteration that gives the estimate of the total transformation as $\mathbf{T}_k = \mathbf{T}'_k * G(\mathbf{x}; \sigma_S)$.

D. Order of computational complexity

The computational cost of pairwise DCE-MRI registration depends on: m-effective size for each of the image dimensions, n-size of a neighborhood window $|N|$, p-spatial subsampling factor between nodes, and of the spatial Gaussian smoothing σ_S. The presented method even when operating in full spatial resolution significantly expedites the non-rigid registration task compared with the B-Splines [4]. In the proposed method the pairwise registration requires the computation and deconvolution of the joint statistics and the spatial smoothing only once per iteration. This is in contrast to the B-Splines method extended with the MI that requires the joint statistics estimation and the spatial smoothing $|N|$ times for each of the $(m/p)^3$ nodes in every iteration to cover an image. The complexity of the proposed method is $O(m^3[n + \sigma_S])$, while that of the B-Splines method is $O(m^3(m/p)^3[n + n\sigma_S])$. The cost of the Demons method extended with MI can be even higher than that of the B-Splines depending on the levels l of the multiresolution pyramids it is often combined with. Assuming that the image widths are halved at every level, the cost is $O\left(m^3\left(\sum_{l'=0}^{l'=l-1}\left(\frac{m}{2^{l'}}\right)^3\right)[n + n\sigma_S]\right)$.

III. Experiments and results

A. Implementation and end condition of iterations

The method has been implemented in *C++*. To improve performance the Wiener filter for the statistics has been implemented separably and is approximated as $f_{i,j} = \frac{G_i}{||G_i||_2^2+\epsilon} * \frac{G_j}{||G_j||_2^2+\epsilon}$ assuming that $G_{i,j} = G_i * G_j$, where G_i and G_j are 1D Gaussian filters. The standard deviation σ_W for the Wiener filter has been set to 2% of the dynamic range and the value of ϵ to 0.1. The spatial regularization of the transformation has been performed using the ITK [8] implementation of the 3D recursive separable Gaussian filter on the components of the displacement u_x, u_y and u_z along the three axes. Both the pairwise non-rigid registration method developed in this work as well as the pairwise non-rigid B-Splines method process 3D+time images and are preceded by the rigid and affine registration methods provided by ITK [8].

The optimization iteratively alternates between the constraints arising from the statistical restoration and from the spatial regularization. The convergence of the registration is evaluated at every iteration. It uses the average L_2 norm of the spatial transformation $||T_k||$. The stop condition s of the iterations is $s = \frac{||T_k||}{||T_0||} - 1 < -1\%$. A maximum number s_{max} of iterations is also enforced.

B. Validation methodology

To evaluate the quality of the registration obtained for real datasets with the method presented, the voxelwise Sum of

Absolute Differences $SAD = \sum_{t=0}^{t=\tau-1} \sum_{\mathbf{x}} |I_{t+1}(\mathbf{x}) - I_t(\mathbf{x})|$ has been calculated within a ROI between consecutive frames before and after the registration. The SAD for the phantom has been calculated between the registered and the ground truth images. The percent improvement (Imp) of SAD is defined as $Imp_{\%} = \frac{SAD_{bef} - SAD_{aft}}{SAD_{bef}} 100\%$, where SAD_{bef} and SAD_{aft} represent the SAD calculated before and after the registration, respectively. The method has been compared with the pairwise B-Splines based non-rigid registration method combined with MI as provided by ITK.

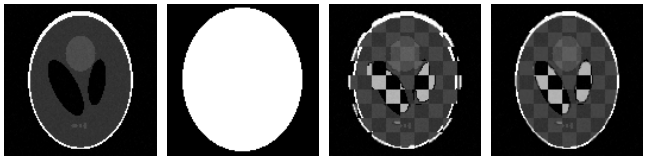

(a) Reference (b) ROI mask (c) Before (d) After

Fig. 2: A 2D section from the 3D registration of simulated volumetric phantom images in an ROI. (c) and (d) are the checkerboard compositions interleaving I_{ref} and I_{mov} before and after the registration, respectively.

C. Datasets description and registration results

A validation data for the proposed method has been applied to two images of a multicontrast simulation with the 3D Shepp-Logan phantom with a full resolution of 128×128×128 pixels as displayed in Fig. 2 which shows an obvious improvement in registration. The phantom has been modified to simulate the contrast enhancement and a sinusoidal function over the spatial image coordinates in all dimensions has been applied to simulate a non-rigid transformation. The value of σ_S has been set to 6 voxels. The registration has been performed in a manually specified ROI of Fig. 2b. After 8 iterations it can be seen in Fig. 2d that the phantom is properly registered. The registration between I_{ref} and I_{mov} gives an $Imp_{\%}$ of about 68%. A performance comparison with the B-Splines method is shown in Table I.

The patient data in this study include liver datasets from 2 patients [9] and lung datasets from 2 patients. All patient datasets were acquired in regular free breathing with an 1.5T MRI scanner (Sonata, Siemens/Erlangen) using a 3D Flash pulse sequence. The images at every time point consist of 20 slices of 128×128 pixels with an in-plane spacing of 3.1mm and a slice thickness of 3.5mm. The scan lasted a total of 6min and produced a time series of 72 images with a time resolution of 5sec. The value of σ_S has been set to 10mm for all axes and for all datasets.

Prostate datasets from 4 patients were also considered and analyzed. They have been acquired with a 3T MRI scanner (TIM-Trio, Siemens/Erlangen) using a 3D Flash pulse sequence. The images at every time point consist of 28 slices of 192×150 pixels with an in-plane spacing of 1.8mm and a slice thickness of 3.5mm. The scan lasted a total of about 7min and produced a time series of 50 images with a time resolution of 8sec. The value of σ_S has been set to 3mm for all axes and for all prostate datasets.

The manually specified ROI for the examples in Fig. 3 are shown in Fig. 3d and 3j. As visual evaluation for the

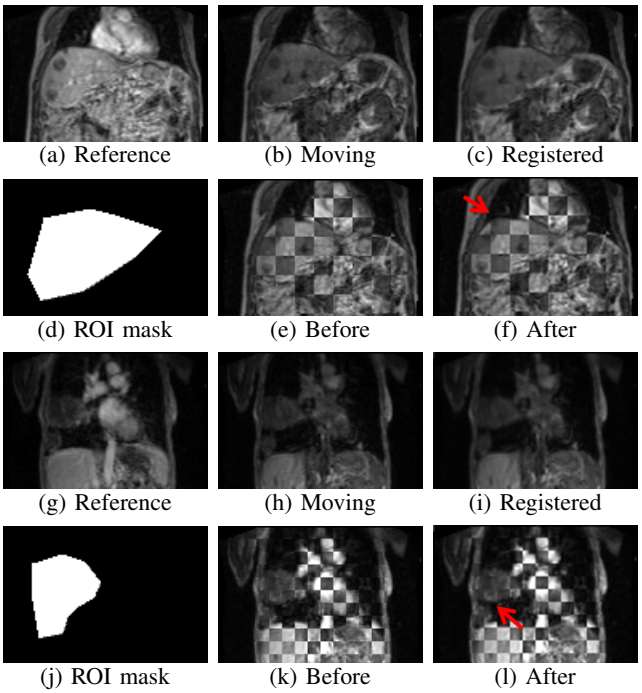

(a) Reference (b) Moving (c) Registered
(d) ROI mask (e) Before (f) After
(g) Reference (h) Moving (i) Registered
(j) ROI mask (k) Before (l) After

Fig. 3: A coronal section from the volumetric registration of a real dataset of a liver (a)-(f) and of a lung (g)-(l). In (f) and (l) the arrow points to a registration improvement.

liver and lungs datasets, a 1D axial window of 15 pixels has been considered. This window is intended to produce kymograms to track the motion of the liver or the lung lesion due to breathing. The colors in the kymograms represent the intensity of pixels showing a separation between the different tissue types. The kymograms of the first example in Fig. 3 are shown in Fig. 4c and 4d and show that the movement due to breathing has been significantly compensated by the registration. The average intensity over time of an ROI which contains only a single lesion has also been calculated as shown in Fig. 4b. Some artifacts non related to motion are still present after the registration. The complete evaluation protocol has been applied to all datasets giving the results shown in Table I.

The tests were performed on a workstation with an Intel Core2 Duo 3.0 GHz CPU, 8GB of RAM. Our initial implementation of the method for a typical image shown in Fig. 3 achieved more than 230% speedup and had a 260% lower working memory requirement compared to the B-Splines method as shown in Table I. It also achieved improvements in resolution by operating in full image resolution as opposed to the B-Spline method that in practice requires subsampling. The B-Splines method tested operates in a grid of size 20×20×20, which implies a resolution of $20 \times 20 \times 3.5mm^3 = 1400mm^3$ as a subsampling in liver and lung datasets. Our method operates in full spatial resolution of $3.1 \times 3.1 \times 3.5mm^3 = 34.2mm^3$, which provides a resolution 41 times higher. The values of $Imp\%$ of the proposed method compared to those of the B-Splines method are shown in Table I.

Datasets	Method	Imp (%)	Resol. (voxels)	Exec. time	Memory Space
Phantom	B-Splines	66.42%	1/262	19min	730MB
	Proposed	68.54%	1	8min	450MB
Liver 1	B-Splines	1.75%	1/41	∼14hrs	650MB
	Proposed	30.81%	1	∼ 6hrs	250MB
Liver 2	B-Splines	34.20%	1/41	∼15hrs	650MB
	Proposed	37.64%	1	∼ 5hrs	250MB
Lung 1	B-Splines	27.18%	1/41	∼11hrs	650MB
	Proposed	33.21%	1	∼ 5hrs	250MB
Lung 2	B-Splines	28.86%	1/41	∼6hrs	650MB
	Proposed	28.51%	1	∼ 4hrs	250MB
Prostate 1	B-Splines	27.96%	1/72	∼11hrs	870MB
	Proposed	29.32%	1	∼ 5hrs	300MB
Prostate 2	B-Splines	21.10%	1/72	∼11hrs	870MB
	Proposed	21.19%	1	∼ 5hrs	300MB
Prostate 3	B-Splines	21.67%	1/72	∼11hrs	870MB
	Proposed	17.71%	1	∼ 5hrs	300MB
Prostate 4	B-Splines	18.84%	1/72	∼11hrs	870MB
	Proposed	19.73%	1	∼ 5hrs	300MB

TABLE I: Comparison of the proposed method with the B-Splines.

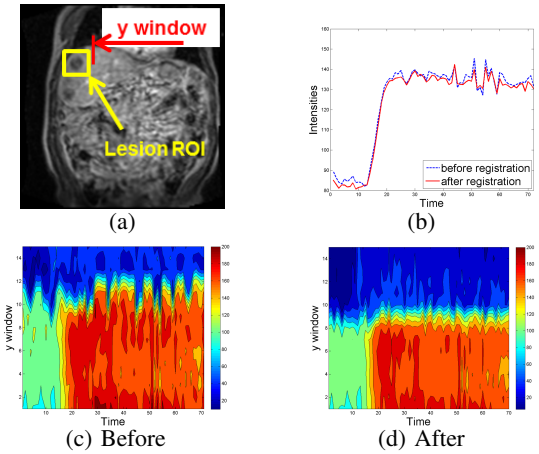

(a) (b) (c) Before (d) After

Fig. 4: In (b) are the time-intensity curves before and after the registration over a lesion ROI. In (c) and (d) are the kymograms resulting from a 1D axial window before and after registration.

IV. Summary and Discussion

The time interval between consecutive images from the real time series of 5 to 8sec is larger than both the breathing cycle as well as the heart beat rate that makes temporal adjacency insignificant. Thus, the pairwise registration of the entire real time series was performed by taking as a reference an image manually selected from the contrast enhanced phase that significantly improves the co-registration. The rigid and affine pre-processing registrations mainly account for the translational component of the breathing motion. The important parameters of the non-rigid registration are the σ_W of the Wiener filter and σ_S of the spatial regularization. The value of σ_W must be smaller than the distance between adjacent tissue distributions in the joint statistics. The value of σ_S must be smaller than the spatial extent of the displacement field. As shown analytically and experimentally in Table I the order of computational complexity is lower than that of the B-Splines based method. The overall speedup is on average approximately 2 to 3 times. That makes the non-rigid registration of a DCE-MRI time series effective and practical and enables the dense spatial registration in a manner robust against contrast changes and anisotropy.

The total time performance of the methods include the common cost of the rigid and affine pre-processing steps. The method developed significantly improves the efficiency and accuracy of non-rigid registration of DCE-MRI datasets while operating densely in full spatial resolution. The method is based on a systematic model of the misregistration and its removal. It has accurately compensated the motion in a phantom as well as in several representative DCE-MRI real datasets. The non-rigid registration can accommodate both same as well as variable image contrasts. It is iterative and results in an effective deconvolution of the joint statistics that only requires a single estimation of the joint statistics and the spatial smoothing per iteration. The registration method does not involve the MI distance measure. The MI allows more degrees of freedom than necessary and leads to a significantly higher computational cost. The performance of this method as well as of all methods based on image statistics is improved if a spatial ROI of meaningful contrast is considered.

Another advantage of the method is that it is robust to the anisotropic resolution present in the clinical imaging data of this study. The robustness of the method has also been shown by evaluating it with datasets from a variety of anatomic regions including liver, lung, and prostate. The resulting time activity curve can also provide pharmacokinetic information.

References

[1] D. Rueckert, L. Sonoda, C. Hayes, D. Hill, M. Leach, and D. Hawkes, "Nonrigid registration using free-form deformations: application to breast MR images," *IEEE TMI*, vol. 18, no. 8, pp. 712–721, 1999.

[2] J. Thirion, "Image matching as a diffusion process: an analogy with Maxwell's Demons," *Med. Image Analysis*, vol. 2, no. 3, pp. 243–260, 1998.

[3] A. Martel, M. Froh, K. Brock, D. Plewes, and D. Barber, "Evaluating an optical-flow-based registration algorithm for contrast-enhanced magnetic resonance imaging of the breast," *Phys. in Med. and Biol.*, vol. 52, no. 13, p. 3803, 2007.

[4] F. Zöllner, R. Sance, P. Rogelj, M. Ledesma-Carbayo, J. Rørvik, A. Santos, and A. Lundervold, "Assessment of 3D DCE-MRI of the kidneys using non-rigid image registration and segmentation of voxel time courses," *Comput. Med. Im. and Graphics*, vol. 33, no. 3, pp. 171–181, 2009.

[5] J. Pluim, J. Maintz, and M. Viergever, "Mutual information matching and interpolation artefacts," in *SPIE Medical Imaging*, vol. 3661, 1999, pp. 56–65.

[6] N. Wiener, *Cybernetics-: or the Control and Communication in the Animal and the Machine*. MIT press, 1965, vol. 25.

[7] M. Schabel, "3D Shepp-Logan phantom," *MATLAB Central File Exchange*, pp. 1–35, 2006.

[8] L. Ibanez, W. Schroeder, L. Ng, and J. Cates, *The ITK Software Guide*, 2nd ed., Kitware, Inc. ISBN 1-930934-15-7, 2005.

[9] S. Steinbild, J. Arends, M. Medinger, B. Häring, A. Frost, J. Drevs, C. Unger, R. Strecker, J. Hennig, and K. Mross, "Metronomic antiangiogenic therapy with capecitabine and celecoxib in advanced tumor patients–results of a phase II study," *Onkologie*, vol. 30, no. 12, pp. 629–635, 2007.